Biochimica et Biophysica Acta 1852 (2015) 1676–1686

Contents lists available at ScienceDirect

Biochimica et Biophysica Acta

journal homepage: www.elsevier.com/locate/bbadis

Dysregulation of clathrin promotes thyroid cell growth and contributes to multinodular goiter pathogenesis

Sin-Ting Lau [a], Tingwen Zhou [a], Jessica Ai-jia Liu [a], Eva Yi-Man Fung [b,c], Chi-Ming Che [b,c], Brian Hung-Hin Lang [a], Elly Sau-Wai Ngan [a,*]

[a] Department of Surgery, Li Ka Shing Faculty of Medicine, University of Hong Kong, Pokfulam, Hong Kong
[b] Department of Chemistry, University of Hong Kong, Pokfulam, Hong Kong
[c] State Key Laboratory of Synthetic Chemistry, Chemical Biology Centre, University of Hong Kong, Pokfulam, Hong Kong

ARTICLE INFO

Article history:
Received 23 January 2015
Received in revised form 6 May 2015
Accepted 7 May 2015
Available online 13 May 2015

Keywords:
TTF1
Multinodular goiter
Proteomics
Proliferation

ABSTRACT

A germline mutation (A339V) in thyroid transcription factor-1 (*TITF1/NKX2.1*) was shown to be associated with multinodular goiter (MNG) and papillary thyroid carcinoma (PTC) pathogenesis. The overexpression of A339V TTF1 significantly promoted hormone-independent growth of the normal thyroid cells, representing a cause of MNG and/or PTC. Nevertheless, the underlying mechanism still remains unclear. In this study, we used liquid chromatography (LC)–tandem mass spectrometry (MS/MS)-based shotgun proteomics comparing the global protein expression profiles of normal thyroid cells (PCCL3) that overexpressed the wild-type or A339V TTF1 to identify key proteins implicated in this process. Proteomic pathway analysis revealed that the aberrant activation of epidermal growth factor (EGF) signaling is significantly associated with the overexpression of A339V TTF1 in PCCL3, and clathrin heavy chain (Chc) is the most significantly up-regulated protein of the pathway. Intriguingly, dysregulated Chc expression facilitated a nuclear accumulation of pStat3, leading to an enhanced cell proliferation of the A339V clones. Down-regulation and abrogation of Chc-mediated cellular trafficking, respectively, by knocking-down Chc and ectopic expression of a dominant-negative (DN) form of Chc could significantly reduce the nuclear pStat3 and rescue the aberrant cell proliferation of the A339V clones. Subsequent expression analysis further revealed that CHC and pSTAT3 are co-overexpressed in 66.7% (10/15) MNG. Taken together, our results suggest that the A339V TTF1 mutant protein up-regulates the cellular expression of Chc, resulting in a constitutive activation of Stat3 pathway, and prompting the aberrant growth of thyroid cells. This extensive growth signal may promote the development of MNG.

1. Introduction

Approximately 200 million people in the world suffer from some form of thyroid disease. Thyroid nodules, thyroid lumps, or an enlargement of the thyroid gland known as goiter are the most common endocrine problem. It is estimated that 4–8% of adult women and 1–2% of adult men have thyroid nodules that could be felt on physical examination, but closer to 30% of women have nodules detectable by ultrasound. Although the majority of thyroid nodules are benign (not cancerous), about 10% of nodules do harbor a cancer. In addition, it is known that about 6% of multinodular goiter (MNG) patients eventually develop thyroid cancer [1–6].

Papillary thyroid carcinoma (PTC) is the most common subtype of thyroid malignancies, accounting for approximately 80% of all primary thyroid cancers. Intriguingly, families with autosomal-dominant inheritance pattern for MNG, PTC, or both strongly suggest the presence of common genetic determinants for MNG and PTC. Previously, our group has identified a germline missense mutation (1016C > T) in *TITF1/NKX2.1* encoding a mutant TTF1 protein (A339V), which may contribute to predisposition for MNG and PTC, further highlighting a genetic link between these two diseases [7]. The ectopic expression of the A339V mutant protein in a normal rat thyroid PCCL3 cell line results in a significant up-regulation of cellular proliferation of these thyroid cells and promotes their thyrotropin (thyroid-stimulating hormone, TSH)-independent growth, which was in part attributed to activated Stat3 survival signal in these cells [7]. Nevertheless, the underlying mechanism for the A339V-associated proliferation remains largely unclear.

In normal thyroid glands, a fine regulation on thyrocyte growth and differentiation is essential to maintain tissue homeostasis; which occurs through complex interactions between TSH and other growth factors

* Corresponding author at: Department of Surgery, University of Hong Kong, Pokfulam, Faculty of Medicine Building, 21 Sassoon Road, Hong Kong, SAR, China. Tel.: +852 3917 9641; fax: +852 3917 9621.
E-mail address: engan@hku.hk (E.S.-W. Ngan).

http://dx.doi.org/10.1016/j.bbadis.2015.05.005
0925-4439/

and cytokines [8]. Among which, epidermal growth factor (EGF) is found synthesized locally, and playing crucial roles in regulation of thyroid proliferation and differentiation [9]. Aberrant EGF signaling is commonly associated with the loss of thyroid specific functions, goiter development, as well as enhanced PTC aggressiveness [9,10]. Similarly, as one of the downstream regulators of the EGF signaling pathway, signal transducers and activators of transcription 3 (STAT3) is found to be highly expressed and activated in the tissue specimens of thyroid cancers, including lymphatic metastasis of PTC [11]. In particular, the activated form of the protein, pSTAT3, is significantly up-regulated in PTC with high metastatic potential [11]. All these evidence suggest that an optimal level EGF-STAT3 signaling must be achieved and cumulative alterations in this signaling pathway may lead to the stepwise transition towards malignancy, including gaining resistance to growth inhibition and ability to proliferate independently on growth factors and to replicate infinitely [12].

Although we have previously identified a missense mutation in *TITF1/NKX2.1* (A339V) as a genetic cause for the predisposition of MNG and PTC, to date, the molecular mechanism(s) underlying this process is still elusive. In this study, we aimed to address this question using a mass spectrometry-based quantitative proteomic approach with our established *in vitro* cell line models. Our quantitative proteomics study has identified proteins that are significantly dysregulated in thyroid cells that expressed A339V TTF1. In addition, with pathway analysis, clathrin heavy chain (Chc) was defined as the most predominant EGF pathway component associated with the aberrant growth of these thyroid cells. Subsequent functional studies further delineated the causal link between A339V mutation, the dysregulation of clathrin-mediated endocytosis (CME), and the aberrant growth of thyroid cells. To further explore the clinical relevance of Chc in MNG and/or PTC pathogenesis, we also examined the expression profiles of CHC and pSTAT3 in MNG and PTC samples from patients carrying wild-type *TITF1*. We showed that elevated Chc is associated with the development of MNG, but not PTC. In summary, with this integrated approach, we have demonstrated that aberrant CME may represent a disease mechanism underlying the development of benign thyroid lesions such as MNG.

2. Materials and method

2.1. Patient samples

A total of 28 pairs of MNG/tumor and the adjacent non-tumor specimens were collected for this study. All subjects enrolled in the study were consecutive unrelated patients with a histological diagnosis of either MNG/nodular hyperplasia ($n = 15$) or PTC ($n = 13$) who underwent a complete thyroidectomy at our institution. For patients with bilateral benign thyroid nodules or multifocal PTC, tumor tissue was taken from the largest nodule while the non-tumor tissue was taken either from the isthmus or the contralateral normal lobe. Fourteen (50%) patients had a clinically palpable or significant goiter at least 12 months before operation. All 13 patients with the diagnosis of PTC belonged to the classic type (i.e. no histological variants of PTC). Patients with clinically occult microcarcinoma were not included. Most of the 28 patients were female (82.1%) and local ethnic Chinese (96.4%). The median ages of the MNG and PTC cohorts were 61 years (range: 30–90 years) and 48 years (range: 8–82 years), respectively. All histological diagnoses were made based on standardized criteria approved by the World Health Organization [13]. None of the patients had past exposure of the head and neck region to ionizing radiation. Ethical approval for this study was obtained from the Institutional Review Board of the University of Hong Kong/Hospital Authority Hong Kong West Cluster (UW 06-369 T/1394). Informed consent was received from each subject.

2.2. Cell lines and stable transfectants

PCCL3 rat thyroid cell line was a gift from Professor Jean-Paul Blondeau, France. Various stable transfectants were generated previously, including PCCL3 stably transfected with the wild-type (pRC/CMV-WT) (a gift from Dr Parviz Minoo, University of Southern California [14]), mutant (pRC/CMV-A339V) TTF1, or empty vector pRC/CMV (Ctrl) (Promega, Madison, WI) [7]. Briefly, cells were maintained in H4 medium, which consisted of Coon's medium with F12 high zinc supplement (Sigma-Aldrich, St Louis, MO) and 5% fetal bovine serum (Invitrogen, Carlsbad, CA), 0.3 mg/mL L-glutamine, 1 mIU/mL thyrotropin (Sigma-Aldrich, St Louis, MO), 10 μg/mL insulin, 5 μg/mL apo-transferrin, 10 nmol/L hydrocortisone, 250 ng/ml G418, and penicillin/streptomycin.

2.3. Liquid chromatography (LC)–tandem MS (MS/MS)

Cell lysates of PCCL3 stable transfectants (WT, A339V and Ctrl) were purified, trypsin digested, and subjected to LC-MS/MS analysis as described in the Supplementary method.

2.4. Cell proliferation assay

For each well in 96-well culture plates, 5×10^3 cells were seeded and cultured for 1 day to allow the cell attachment. The cell proliferation rate was measured using the colorimetric Cell Proliferation ELISA kit (Roche, Indianapolis, IN) in the presence or absence of Stat3 inhibitor (100 μM). In brief, a 1 μM solution of BrdU was added to the cell culture 4 h before the assay. After the incubation hours, cells were fixed, blocked, and incubated with anti-BrdU antibody according to the manufacturer's protocol.

For the overexpression/knockdown experiments, cells were first transfected with pEGFP-C1-Chc(1-479), pCMV-EGFP (a gift from Professor Steven J. Royle, University of Liverpool, UK), non-silencing (*NS*) *siRNA* (5′-UUCUCCGAACGUGUCACGUUU-3′), or *si-Chc* (5′-AGGACCUU CAGAAGGGCGAUU-3′) with/without GFP-CHC17KDP (Addgene, Plasmid #59799). Cell proliferation analyses were performed at 48 h after transfection. Three independent experiments were performed with the selected stable transfected clones, and each experiment was performed in triplicates.

2.5. Immunoblotting

To examine the expression of the target proteins in the patient tissues and stable transfectants, tissues or cells were lysed. Cell lysates containing 10–30 μg of total or fractionated (cytoplasmic or nuclear faction) protein were separated on 10 % sodium dodecyl sulfate–polyacrylamide gels and blotted onto nitrocellulose membranes. The membranes were then incubated with primary antibodies listed in Supplementary Table 1. The same membranes were probed with anti-β-actin, anti-β-tubulin, or anti-histone antibody to ensure equal loading of cell protein per lane. All blots were incubated with secondary horseradish peroxidase-conjugated antibody. Antibody-bound proteins were visualized using a chemiluminescence system (Amersham Biosciences, Piscataway, NJ).

For examining Egfr recycling, cells were cultured in serum free Coon's medium for 6 h before addition of EGF. Cells were harvested at 0, 30, and 90 min after addition of EGF (100 ng/ml) with or without pretreatment with choroquine (100 μM for 3 hrs at 37 °C).

2.6. Immunocytochemistry

Stable transfectants (3×10^4 cells per well in 24-well plate) were seeded on poly-D-lysine coated coverslips. Some of the wells were subjected to transient transfection with either pEGFP-C1-Chc(1-479) or pCMV-EGFP for 24 h prior to harvesting and fixation. After 4 % paraformaldehyde fixation, cells were blocked with 1% bovine Serum albumin

in PBS with or without 0.1% triton for 1 h and incubated overnight with polyclonal antibody against Chc or pStat3 at 4 °C. The cells were subsequently washed with PBS and further incubated with Alexofluor secondary antibodies for 2 h at room temperature in dark. Vectashield® with DAPI (Vector Laboratories, Inc., Burlingame, CA) was used as the mounting medium. Signals were detected, and images were captured with a Nikon Eclipse 80i upright Fluorescence microscope (Nikon, Melville, NY).

2.7. Luciferase reporter assay

Cos-7 cells (3×10^4 per well in 24-well plate) were transfected with 250 ng of a reporter plasmid that encoded firefly luciferase under the control of the *Chc* promoter of different length, 50 ng of a reporter plasmid that encoded *Renilla* luciferase under the control of the SV40 promoter (pRL-SV40), and 400 ng of the WT (pRc/CMV-WT) or mutant (pRc/CMV-A339V) TTF1 expression plasmid or empty vector (pRc/CMV) to compare the ability of WT and A339V to transactivate the *Chc* promoter. Luciferase reporter assays were carried out using the Dual-Luciferase Reporter Assay System (Promega) according to the manufacturer's protocol. Twenty-four hours after transient transfection, cells were washed once with phosphate-buffered saline and harvested in 50 μL passive lysis buffer (Promega). Luminescence measurements were made on 10 μL of each sample lysate with a Microplate Luminometer LB96V (Berthold Technology, Bad Wildbad, Germany). Firefly luciferase activity was normalized against *Renilla* luciferase activity to correct for variations in transfection efficiency.

2.8. Electrophoretic mobility shift assay (EMSA)

The interaction of WT and A339V with the Chc promoter was assessed using EMSA. Chc promoter DNA (1kp) was amplified with TaqGold polymerase using primer pairs Rat CHCpromo-F5 (5′-CTGCGGTACCCGTCAGAAGGGGCGTGCGTCA-3′) and Rat CHCpromo-R (5′-CTGCACGCGTGGCCGCTAGCTTCCTTCCCA-3′) and annealing temperatures of 56 °C. EMSAs were performed using the Electrophoretic Mobility Shift Assay kit (Invitrogen) according to the basic protocol supplied by the manufacturer. In brief, protein–DNA samples were then incubated on ice for 30 min in 1 × binding buffer (700 mM KCl, 2.5 mM DTT, 2 mM EDTA, 25 mM Tris-HCl, 10 mM MgCl2, and 2% glycerol). The samples were run on a 5% TBE nondenaturing polyacrylamide gel in 0.5× TBE buffer before being stained with SYBR® Green for 30 min to stain for DNA and imaged on Syngene G:Box followed by 3 h of staining with SYPRO® Ruby followed by destaining and imaging on Syngene G:Box to monitor for the colocalization of DNA and protein in shifted bands.

2.9. Statistical analysis

Fisher's exact test was used for comparison of dichotomous variables and the Mann–Whitney *U*-test was used for continuous variables between groups. Continuous clinical variables were expressed as median (range). Statistical analysis was performed using the SPSS statistics software package (SPSS, Chicago, IL). Statistical comparisons for the cell proliferation rates among the three groups of stable cell lines were done by one-way ANOVA followed by Tukey post-test. All experiments were performed with at least three samples per group, and results were derived from at least three independent experiments. Experimental data were expressed as mean values ± SEM. Statistical analysis was performed using the GraphPad Prism 5 (GraphPad Software, San Diego, CA). Unless otherwise specified, comparison between any 2-treatment groups was analyzed by Student *t*-test. A *p*-value less than 0.05 was interpreted to represent a statistically significant difference.

3. Results

3.1. Proteomic pathway analysis reveals up-regulation of EGF pathway in PCCL3 that overexpressed with A339V TTF1

To elucidate the potential molecular effects upon the expression of mutant A339V TTF1 in PCCL3, LC-MS/MS-based shotgun proteomics were performed to compare the global protein expression profiles of rat normal thyroid cell lines (PCCL3) that overexpressed the WT or A339V TTF1 or that contained an empty vector as a control (Ctrl). After excluding single spectrum-matched proteins, comparative proteomic analysis revealed that twenty-three and thirty-seven proteins are differentially expressed in PCCL3 that overexpressed A339V TTF1, when compared to that of WT and the control (Ctrl) clone. A label-free quantitative approach was employed, and the relative abundance was based on the sum of total fragment ion intensities of peptides matched in WT, A339V, and Ctrl clones. The identities and relative abundance of the differentially expressed proteins are summarized in Table 1 and Supplementary Table 2.

A full list of proteins identified from each sample along with their accession numbers and abundances was uploaded to ExPlain™. Proteins were automatically converted to corresponding gene identifications upon data uploading, which were then mapped to upstream key nodes in cellular pathways. To combine the results for the comparisons, a score (S) was calculated for each pathway by combining both the information of up- and down-regulated pathways. The identified pathways were binned according to their scores (S) and plotted as a bar chart (Fig. 1A, sample). The up-regulated pathways were indicated by positive score, while the down-regulated pathways were indicated by negative scores. As shown in Fig. 1A, the histogram was sigmoid and almost symmetric, suggesting that the distribution of these Scores is normal. To determine if the calculated score could be resulted by chance, the threshold value of score (S_0) was accessed by randomizing the ranks of the pathways and calculated the score with the same formulae as the real data (Fig. 1A, random). Again, the S_0 were found distributed normally and symmetrically, and it was highly comparable to that of the samples. Then we used S_0 as a reference to identify the pathways that were significantly different among samples. Those pathways with a score larger than the positive threshold value were considered as significantly up-regulated; pathways with a score smaller than the negative threshold value were considered as significantly down-regulated. The *p*-value of each pathway could be deduced as follows: $p\text{-value} = 10^{-(S - S0)}$. Reasonably, a low *p*-value can be obtained by two replicates for each sample using this cross pairwise comparisons method (Supplementary method).

Comparisons of two pathway analyses were performed: A339V vs WT TTF1 PCCL3 transfectants and WT vs PCCL3 transfected with empty vector (Ctrl). Two significantly up-regulated pathways and 5 significantly down-regulated pathways were consistently detected in both A339V clones C1 and C2. When we compare A339V C1 with WT, EGF pathway came up with the highest score (11.36) being rank 1 in 4 out of 4 comparisons, with a *p*-value of 1.35×10^{-7}. The experiment was repeated with another individual clone of mutant (A339V C2) that gave similar results, with a score of 10.76 and a *p*-value of 4.23×10^{-6} (Fig. 1A). Intriguingly, when we performed an additional control experiment by comparing the pathway results of the Ctrl and that of the WT-TTF1-transfected PCCL3, we found that EGF pathway is slightly down-regulated in cells overexpressing WT-TTF1 with a score and a *p*-value of -6.16 and 2.84×10^{-2}, respectively (Fig. 1B). These data support the notion that TTF1-mediated down-regulation of EGF pathway is essential for thyroid cell differentiation, and this process may be interrupted in patients carrying mutant TTF1.

With our MS data, multiple proteins associated with the EGF pathway were identified as differentially expressed in A339V and WT clones, including clathrin heavy chain (Chc), synthetic high osmolarity-sensitive-1 (Flna), Ras related C3 botulinum toxin substrate-1 (Rac1),

Table 1
Complete list of proteins that are differentially expressed in A339V and TTF1 overexpressing cells.

Accession	Gene	Description	Coverage	No. peptide	Score	A339V	WT	log2 [A339V/WT]
IPI00214582	LOC497813	40S ribosomal protein S7	21.65	3	14.06	251481	2951	6.41
IPI00958405	LOC100362830	Ribosomal protein S7-like	24.64	4	23.09	251481	2951	6.41
IPI00203358	Ppp1cc	Isoform Gamma-1 of serine/threonine-protein phosphatase PP1-gamma catalytic subunit	8.98	2	14.67	1259263	233714	2.43
IPI00203390	Ppp1cb	Serine/threonine-protein phosphatase PP1-beta catalytic subunit	8.87	2	14.67	1259263	233714	2.43
IPI00208265	Ppp1ca	Serine/threonine-protein phosphatase PP1-alpha catalytic subunit	8.79	2	14.67	1259263	233714	2.43
IPI00231715	Ppp1cc	Isoform Gamma-2 of serine/threonine-protein phosphatase PP1-gamma catalytic subunit	8.61	2	14.67	1259263	233714	2.43
IPI00368473	Numa1	Nuclear mitotic apparatus protein 1	9.70	17	24.86	587092	165278	1.83
IPI00766825	Numa1	Nuclear mitotic apparatus protein 1 isoform 2	9.78	17	24.86	587092	165278	1.83
IPI00208917	Aldh7a1	Alpha-aminoadipic semialdehyde dehydrogenase	18.74	8	18.82	538662	173685	1.63
IPI00212697	Napsa	Napsin A aspartic peptidase	6.90	3	15.98	603828	221076	1.45
IPI00212989	Olah	S-acyl fatty acid synthase thioesterase, medium chain	11.41	2	6.73	307333	120351	1.35
IPI00364865	Tex10	Uncharacterized protein	4.20	3	6.37	147813	58964	1.33
IPI00189074	Pabpc1	Polyadenylate-binding protein 1	17.92	10	34.92	289658	118827	1.29
IPI00213463	Actn4	Alpha-actinin-4	31.39	23	74.97	1894923	868125	1.13
IPI00231506	Pgam2	Phosphoglycerate mutase 2	18.18	6	25.36	392540	183683	1.10
IPI00209082	Actn1	Alpha-actinin-1	28.03	19	73.44	2075142	980540	1.08
IPI00454431	Actn1	Brain-specific alpha-actinin 1 isoform	29.10	20	77.16	2075142	980540	1.08
IPI00949794	Actn1	Actn1 protein	28.18	19	73.44	2075142	980540	1.08
IPI00951030	Actn1	100 kDa protein	28.84	19	73.44	2075142	980540	1.08
IPI00193983	Cltc	Clathrin heavy chain 1	19.76	24	80.15	1359887	657720	1.05
IPI00776558	Cltc	Uncharacterized protein	19.71	24	80.15	1359887	657720	1.05
IPI00193279	Oat	Ornithine aminotransferase, mitochondrial	31.66	10	61.58	345820	697622	−1.01
IPI00363236	Lars	Leucyl-tRNA synthetase	7.04	6	15.27	250663	534731	−1.09
IPI00454293	Serinc1	LRRGT00191	2.90	4	13.54	208685	449773	−1.11
IPI00776730	LOC316460	Uncharacterized protein	5.98	15	25.86	2409500	5234776	−1.12
IPI00957757	LOC316460	Uncharacterized protein	5.80	14	23.35	2409500	5234776	−1.12
IPI00209690	Ephx1	Epoxide hydrolase 1	15.82	5	16.17	270774	676355	−1.32
IPI00215277	Pdzd2	PDZ domain-containing protein 2	4.81	9	22.75	1167793	3058996	−1.39
IPI00779574	Pdzd2	280 kDa protein	5.04	9	22.75	1167793	3058996	−1.39
IPI00768895	LOC690147	Epoxide hydrolase 1	19.94	4	12.23	156468	461532	−1.56
IPI00951179	LOC690147	51 kDa protein	14.03	4	12.23	156468	461532	−1.56
IPI00339124	Atp1b1	Sodium/potassium-transporting ATPase subunit beta-1	19.41	5	23.66	672203	2057873	−1.61
IPI00421500	Hnrnpa1	Heterogeneous nuclear ribonucleoprotein A1	21.88	6	36.96	144327	456800	−1.66
IPI00780243	Hnrnpa1	Uncharacterized protein	13.43	4	27.37	144327	456800	−1.66
IPI00781944	Hnrnpa1	Uncharacterized protein	18.77	6	35.28	144327	456800	−1.66
IPI00231502	Ap2b1	Isoform 2 of AP-2 complex subunit beta	8.73	6	17.49	60055	473556	−2.98
IPI00389753	Ap2b1	Isoform 1 of AP-2 complex subunit beta	8.86	6	17.49	60055	473556	−2.98

and Ras homolog gene family member A (RhoA) (Fig. 1C). Among which, Chc was the most significantly up-regulated candidate in both A339V clones (A3399V C1: 2.38 folds; A339V C2: 3.07 folds) when compared to PCCL3 that overexpressed with WT-TTF1.

3.2. Dysregulation of Chc and EGF receptor recycling in A339V PCCL3 cells

To validate the proteomics data, the expression of Chc protein in A339V PCCL3 was examined using immunoblotting (Fig. 2A) and immunocytochemistry (Fig. 2B), in which two independent clones of A339V, WT and Ctrl, were included. In concordant with our proteomics data, expression levels of Chc in A339V clones were higher than that of the Ctrl and WT clones, where Chc is mainly expressed in cytoplasm of these cells. It has been shown that clathrin-dependent endocytosis (CME) prolongs the duration of EGF signaling by sustaining Egfr recycling [15]. Therefore, we also monitored the Egfr degradation and recycling processes in WT-TTF1 and A339V-transfected PCCL3. As illustrated in Fig. 2C, 90 min after addition of EGF, Egfr was completely degraded in WT-TTF1-transfected PCCL3. In A339V PCCL3, the recycling process happened much faster, and a complete degradation was observed in 30 min, wherein we could detect Egfr expression again at 90 min. More importantly, when chloroquine was added into the cultures to inhibit CME by affecting the function of clathrin and clathrin-coated vesicles, the Egfr degradation was abolished is in both A339V and WT-TTF1-transfected PCCL3, suggesting that the Egfr degradation/recycling is clathrin dependent. Taken together, the ectopic overexpression of A339V TTF1 would prolong EGF signaling by sustaining the CME-dependent Egfr recycling.

3.3. Activation of Stat3 pathway promotes cell proliferation of A339V TTF1 PCCL3 cells

Depending on different cellular contexts, EGF pathway typically promotes cell survival, growth, and tumorigenesis, through the activation of AKT/PKB or/and Src/STAT3 downstream signaling. The constitutive activation of Stat3 (Ser727) has been previously identified as the predominant survival signaling pathway for the A339V-associated proliferation [7]. In addition, clathrin also represents a key trafficking component for cytoplasmic transport of pStat3 from cell membrane to perinuclear region [16,17]. Therefore, it is conceivable that up-regulated levels of Chc may also promote the nuclear accumulation of pStat3 (Ser727) in A339V clones. Immunoblotting results with lysates of various stable clones indicated that A339V clones with higher Chc expression have significantly higher amount of total pStat3 (Fig. 3A) and nuclear pStat3 (Fig. 3B), while the Stat3 levels remained similar to those of WT and Ctrl clones (Fig. 3A). Consistent results were observed from immunofluorescence images (Fig. 3C) in which pStat3 were highly expressed in nuclei of these A339V-transfected PCCL3 cells. In contrast, both Ctrl and WT clones showed less Chc (Fig. 3C) and pStat3 staining (Fig. 3C). Furthermore, the nuclear accumulation of pStat3 likely contributes to the A339V-associated proliferation of PCCL3 cells because the proliferation rate of these cells was significantly reduced when a

A

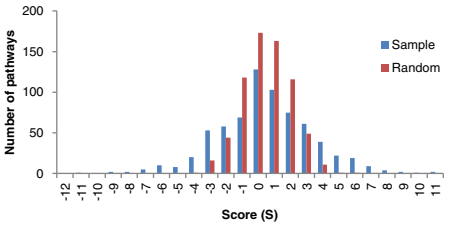

Significantly up-regulated pathways	A339V C1 Score (S)	A339V C1 *p*-value	A339V C2 Score (S)	A339V C2 *p*-value
EGF pathway	11.36	1.35E-07	10.76	4.23E-06
p53 pathway	8.09	2.55E-04	8.25	1.37E-03

Significantly down-regulated pathways	Score (S)	*p*-value	Score (S)	*p*-value
NGF---p75NTR → p50:RelA-p65	-7.07	3.32E-03	-7.55	5.08E-04
IL-1 pathway	-8.58	1.02E-04	-7.96	1.99E-04
Parkin associated pathways	-7.04	3.56E-03	-9.32	8.62E-06
TLR4 pathway	-8.63	9.11E-05	-9.98	1.90E-06
Neurotrophic signaling	-11.36	1.68E-07	-11.36	7.88E-08

B

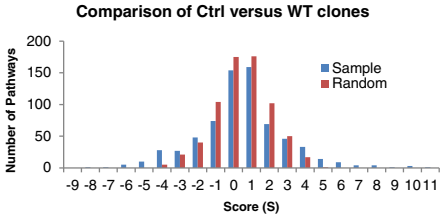

Significantly up-regulated pathways	Score (S)	*p*-value
neurotrophic signaling	10.31	4.24E-06
stress-associated pathways	9.75	1.55E-05
TLR4 pathway	9.17	5.80E-05
IL-1 pathway	9.02	8.37E-05
TLR3 pathway	8.10	6.81E-04
JNK pathway	7.70	1.73E-03
IL-1beta → p50:RelA	7.64	2.00E-03
NGF---p75NTR → p50:RelA-p65	7.17	5.89E-03
LPS → NF-kappaB	7.14	6.25E-03

Significantly down-regulated pathways	Score (S)	*p*-value
IFNalpha,IFNbeta,IFNgamma → Rap1	-6.03	3.80E-02
EGF pathway	-6.16	2.84E-02
insulin pathway	-6.17	2.79E-02
RhoA pathway	-6.20	2.60E-02
PRL pathway	-6.43	1.53E-02
tuberin pathway	-7.44	1.48E-03
IFN pathway	-8.27	2.20E-04

C

Protein	Gene symbol	Protein accession number	Fold change (relative to WT) A339V C1	Fold change (relative to WT) A339V C2
Clathrin heavy chain Hc	Cltc	IPI00193983, IPI00776558	2.38	3.07
Synthetic high osmolarity-sensitive 1	Flna	IPI00409539	1.78	2.05
Ras related C3 botulinum toxin substrate 1	Rac1	IPI00422092, IPI00780227	1.84	2.09
Ras homolog gene family member A	Rhoa	IPI00201699	1.88	1.54

Fig. 1. Proteomic pathway analysis reveals that EGF pathway is significantly up-regulated in A339V TTF1 PCCL3. (A) Pathway analysis comparison for A339V versus WT clones. Pathway analysis was performed using Pathway Search Engine in combination with ExPlain™ software. Upper panel: Histogram shows normal distributions of Score (S) for the samples and the threshold value of score (S_0). Lower panel: Proteins associated with the EGF pathway were significantly up-regulated in A339V relative to WT clones. (B) Pathway analysis comparison for WT and Ctrl clones. Proteins were identified and compared as in panel A. (C) Deregulated EGF pathway proteins identified in A339V clones.

Stat3 pathway inhibitor, S3I, was added. Furthermore, this was only observed in A339V clones, but not in PCCL3 cells transfected with empty vector (Ctrl) or wild-type TTF1 (WT) (Fig. 3D).

3.4. Chc mediates cellular trafficking of pStat3 in A339V clones

Although the cellular trafficking roles of Chc are well established, Chc has recently been shown to promote mitosis by directly modulating the mitotic spindle. To specifically address whether Chc contributes to the A339V-associated proliferation through its cellular trafficking and/or the mitotic function, the endogenous function of Chc was abolished by two approaches: (1) down-regulation of Chc with *siRNA* or (2) overexpression of a construct encoding only the N-terminal domain (amino acid 1-479) of Chc, which encodes a dominant-negative (DN) form of Chc to specifically prohibit its cellular trafficking function [18]. Immunoblotting results indicated that knockdown of Chc by *siRNA* profoundly reduced nuclear pStat3 and total Stat3, which are accompanied by an accumulation of cytoplasmic pStat3 (Fig. 4A). Importantly, the cell proliferation rates of the A339V C1 and C2 clones were significantly dropped at 48 h post-transfection, and the inhibitory effect of *si-Chc* could be recused by the overexpression of wild-type Chc (Fig. 4B). These data indicated that elevated Chc directly contributes to the increased cellular proliferation rates observed in A339V clones. Similarly, the overexpression of the DN Chc also reduced nuclear pStat3, accompanied by an accumulation of cytoplasmic pStat3. However, in this case, the total Stat3 was not affected (Fig. 4C). In regards to the cell proliferation, the ectopic expression of DN Chc significantly decreased cell proliferation rates of A339V clones and that reached back to the level similar to those of both the Ctrl and WT clones (Fig. 4D). These indicated that the elevated cellular proliferation rates observed in A339V clones are attributed to the subcellular trafficking function of Chc. Taken together, the elevated expression of Chc in A339V clones could favor nuclear localization of pStat3 protein and hence activate its downstream survival signaling, leading to increased cell proliferation rates.

3.5. A339V TTF1 aberrantly transactivates Chc in PCCL3

We next elucidated how A339V TTF1 induces Chc expression. It is noteworthy that A339V mutation is not residing in any of known functional domains for DNA binding or transactivation activity of TTF1, but A339V mutant still exhibits defect on binding onto its consensus regulatory sequence to activate its target gene expression. Therefore, we speculated that A339V TTF1 still retains its transactivation activity, while the A339V mutation on TTF1 may lead to the loss of promoter-specific DNA binding of TTF1. It could result in a random binding to the *Chc* promoter and a dysregulated transactivation of *Chc*. To test our hypothesis, we first evaluate the mRNA level of *Chc* in the stable clones by real-time quantitative PCR. While those of the Ctrl and WT clones remained at relatively similar levels, the average *Chc* mRNA level in A339V clones was found significantly higher than that of the Ctrl and WT clones by approximately 2 folds (Fig. 5A), suggesting enhanced Chc expressions observed in A339V clones were due to alterations at transcriptional level. We then used a two-tier approach to locate the binding site: we first used rVISTA to search for the putative TTF1 binding motif. rVISTA combines searching the major transcription binding site database TRANSFAC Professional from Biobase with a comparative sequence

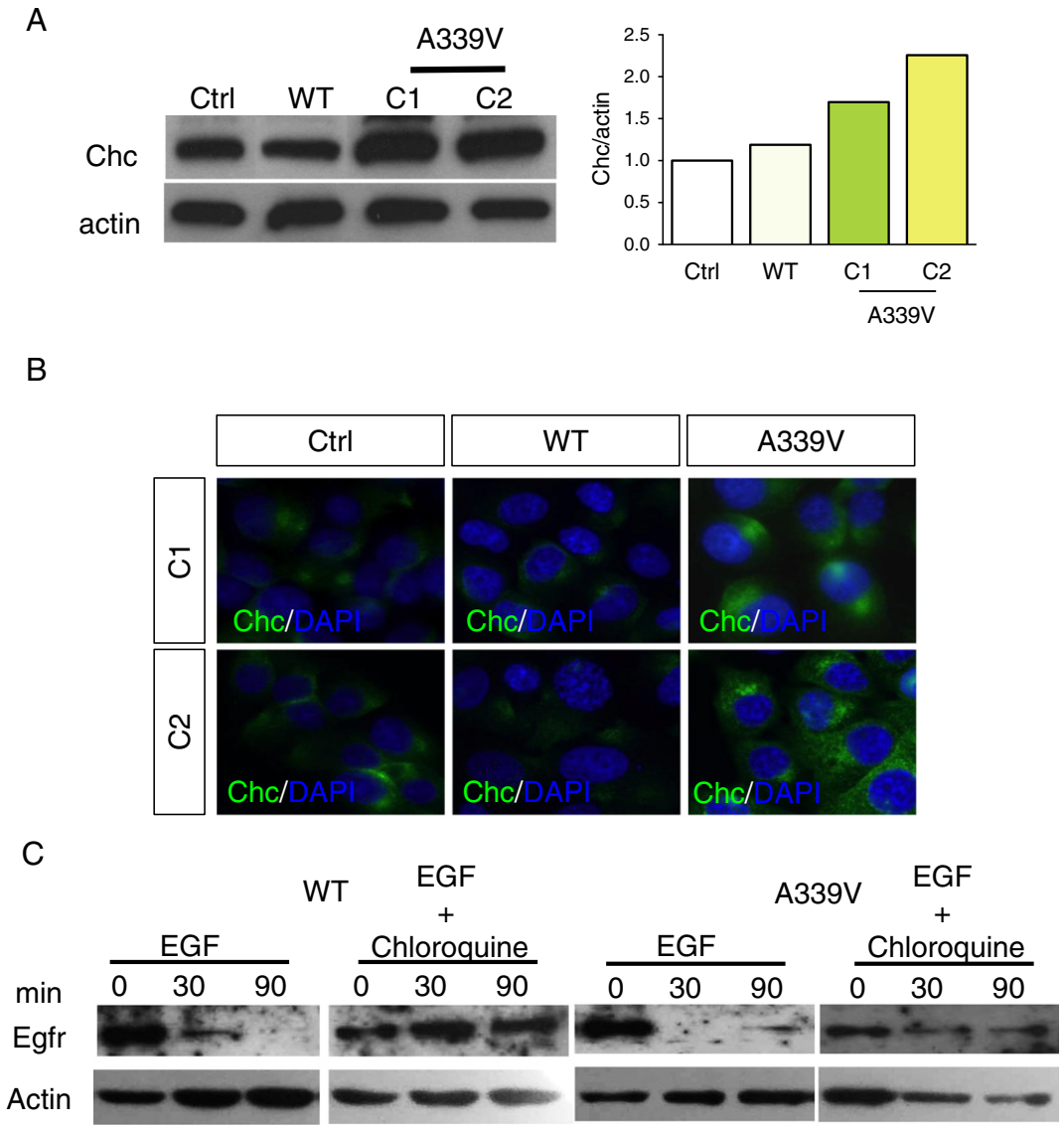

Fig. 2. Elevated expression of Chc and Egfr recycling in A339V clones. (A) Immunoblotting was performed for evaluating the relative protein abundance of Chc in the PCCL3 transfectants (PCCL3 transfected with pRC/CMV (Ctrl), pRC/CMV-TTF1 (WT),and pRC/CMV-A339V TTF1 (A339V)). Actin was used as the loading control. The intensities of the bands were quantified and the normalized values are shown in the bar chart. (B) Immunocytochemistry analysis was performed to examine the cellular localization of Chc in PCCL3 transfectants. Representative images are shown (magnification, ×400). Note that elevated Chc expression was observed in clones overexpressing mutant TTF1 (A339V) when compared to the clones expressing vector (Ctrl) or wild-type (WT) TTF1. (C) Cells were treated with choroquine (100 μM for 3 hrs at 37 °C) and EGF (100 ng/ml) as indicated. Western blot analysis was performed to detect Egfr expression.

analysis to minimize the false positive. There were several putative "TTF1 binding sites" in the *Chc* minimal promoter. Given that previous functional studies from us and the others showed that CAAG … CTTG is the TTF1 core consequence sequence identified in the thyroid (*Tg* promoter) [7] and lung (SFTPA1 promoter) [19] cells, we limited our search with this sequence and no CAAG … CTTG was found in the *Chc* minimal promoter. To further demonstrate that the dysregulated Chc expression is due to the aberrant transactivation by mutant TTF1, luciferase report assays were performed. We transfected Cos-7 with a plasmid encoding firefly luciferase under the control of *Chc* promoter containing either 1 kb or 2 kb proximal promoter sequence (pGL3-Chc), expression vectors for WT (pRc/CMV-WT) or A339V TTF1 (pRC/CMV-A339V), or the control empty vector (pRc/CMV-WT), and with a plasmid encoding *Renilla* luciferase (pRL-SV40). The extent to which TTF1 transactivates the *Chc* promoter was assessed by normalizing firefly luciferase activity to *Renilla* luciferase activity. The basal promoter activities of the 1 kb and 2 kb *Chc* promoters are comparable. The overexpression of WT-TTF1 did not further increase the promoter activity of the *Chc*, and the relative luciferase activities were found similar in both cells transfected with WT TTF1 and control empty vector. In contrast, the overexpression of A339V TTF1 resulted in significant increases in the promoter activities of both 1 kb and 2 kb *Chc* promoters by 2.01 ± 0.76 and 2.29 ± 0.12 folds, respectively (Fig. 5B). In the subsequent gel mobility shift assay, distinct bands were observed with the WT and A339V PCCL3 nuclear proteins (Fig. 5C, nuclear stain). These bands were specific because there was a dose-dependent increase in the amount of proteins that bind on the proximal 1 kb *Chc* promoter (Fig. 5C, protein stain). Together with the data from the luciferase reporter assays, the mutant TTF1 aberrantly transactivates *Chc* gene and the putative binding site for A339V TTF1 is likely located within the proximal 1 kb of the *Chc* promoter.

3.6. Elevated Chc and pSTAT3 expression in MNG

Our previous study showed that patients harboring A339V *TITF1* developed both MNG and PTC and it is not clear whether Chc itself is implicated in the development of MNG, PTC, or both. To assess the

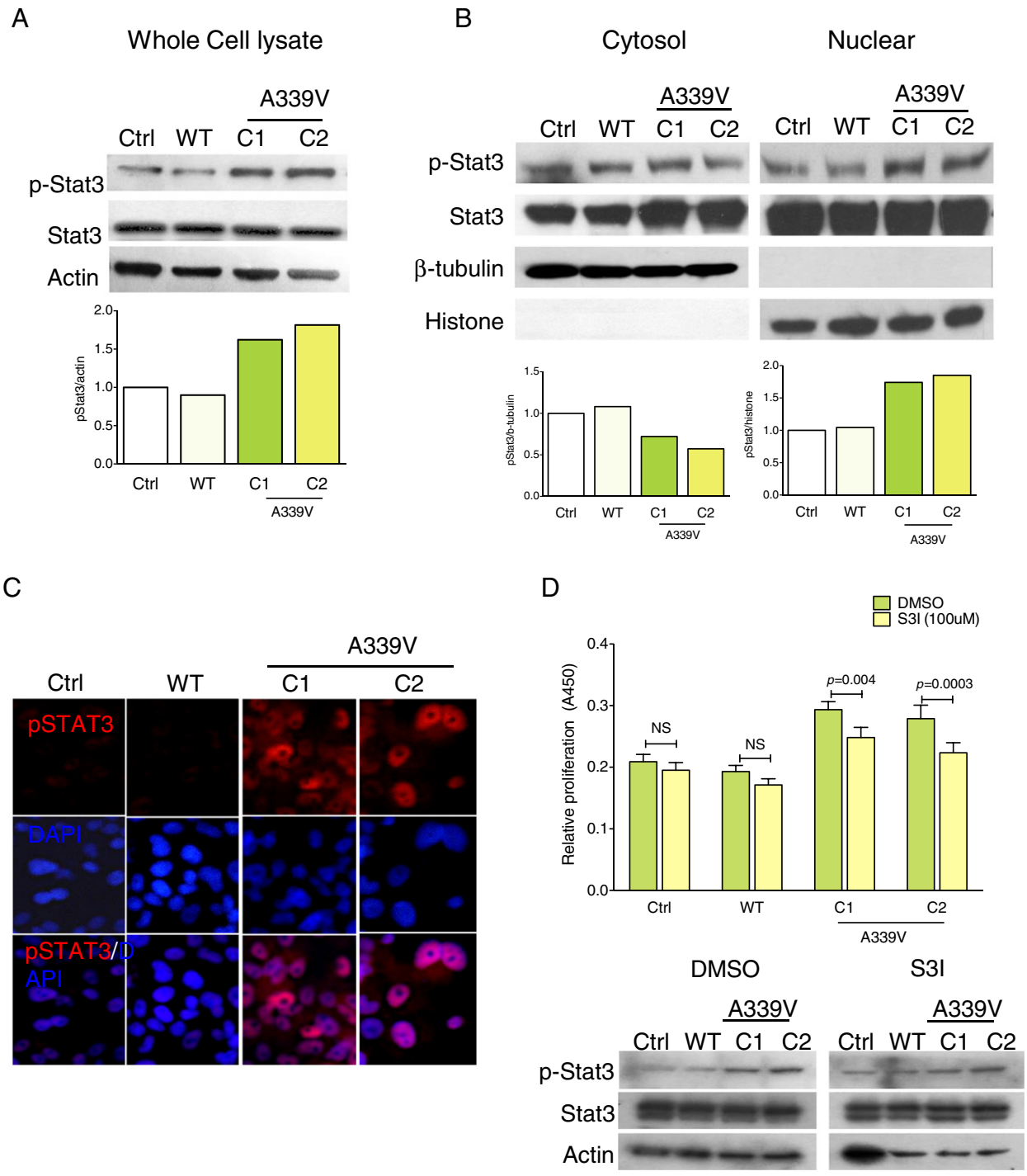

Fig. 3. Elevated expression of Chc is associated with nuclear accumulation of pStat3. Western blot analysis was used to evaluate the levels of p-Stat3, total Stat3 in the (A) whole cell lysate. Actin was used as loading control; (B) the cytoplasm (Cyto) or nucleus (nuclear) of PCCL3 transfectants. β-Tubulin and histone were used as the loading controls for the cytoplasmic and nuclear proteins, respectively. The intensities of the bands were quantified and the normalized values are shown in the bar chart. (C) Immunocytochemistry analysis was performed to localize pStat3 in PCCL3 transfectants. Representative images are shown (magnification, ×400). Note that elevated nuclear accumulation of pStat3 was observed in the A339V clones, while pStat3 was expressed at lower level in PCCL3 cells transfected with pRC/CMV (Ctrl) and pRC/CMV-TTF1 (WT). (D) BrdU cell proliferation assay was performed on cells treated with control vehicle (DMSO) or Stat3 inhibitor, S3I (100 μM). Relative proliferation rates of these cells are shown in the bar chart. *p* values less than 0.05 were deemed to be statistically significant. NS: not significantly different. Western blot analysis was used to evaluate the levels of p-Stat3, total Stat3 in cells treated with DMSO or S3I. Actin was used as loading control.

potential implication of CHC (independent of *TITF1* mutation), we examined CHC expression levels in 15 resected MNG and 13 primary PTC tumors from patients who carry wild-type *TITF1* using Western blotting. Increased CHC expression was detected in 11 of the 15 MNG samples (73.3%, marked by "*"), and no CHC expression was detected in the 13 PTC tumor samples (0.0%) ($p < 0.001$, Fisher's exact test) compared with matched adjacent thyroid/non-tumor tissue samples (Fig. 6). Intriguingly, among these 11 MNG samples with elevated CHC expression, 10 of them also exhibited increased pSTAT3 expression. These data have highlighted the potential link between the elevated

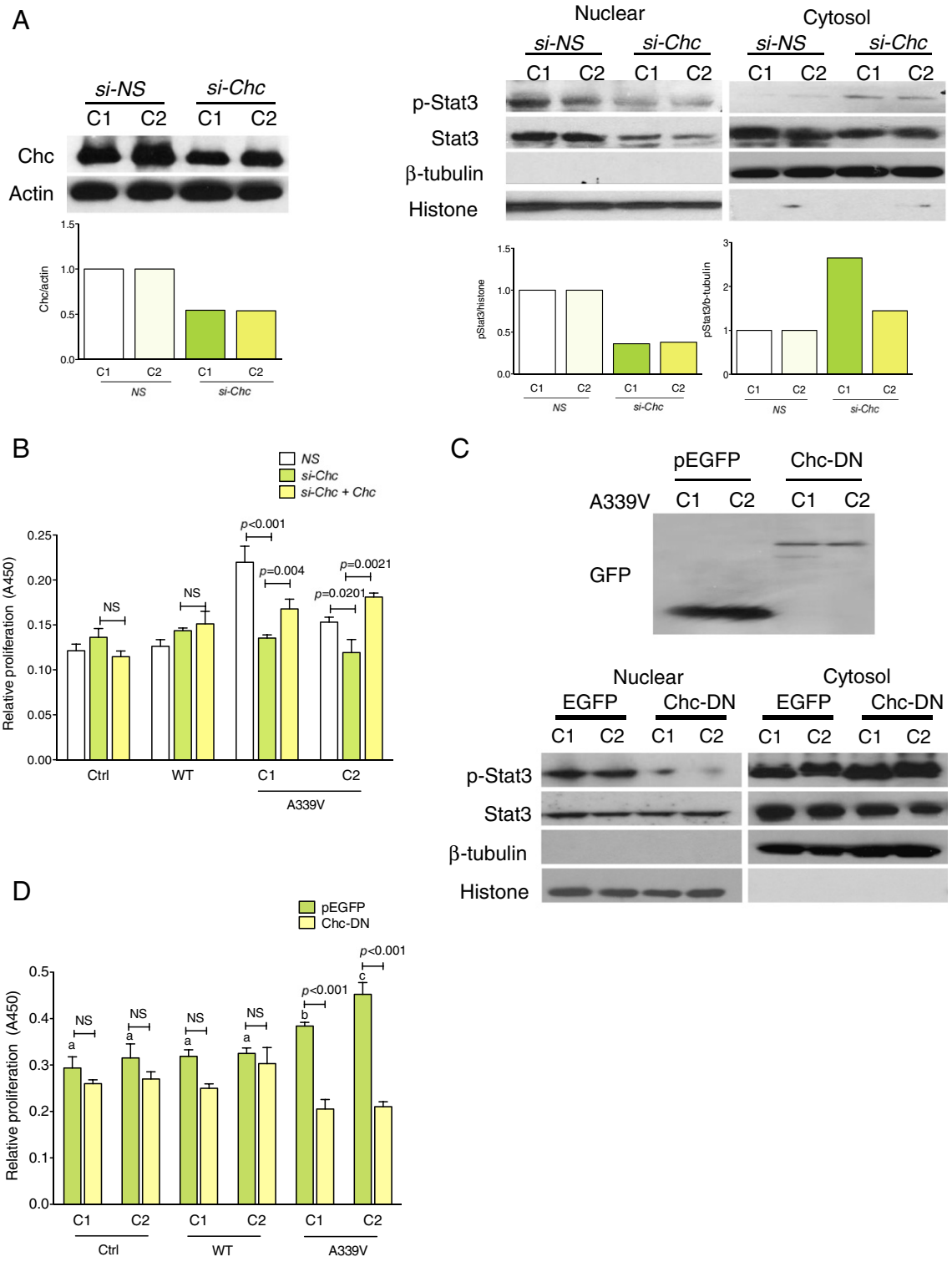

Fig. 4. Elevated expression of Chc enhances cell proliferation of A339V clones by promoting CME-dependent nuclear localization of pStat3. (A) Specific siRNA against Chc (*si-Chc*) or non-silencing siRNA (*si-NS*) were transfected into A339V PCCL3. Western blot analysis was performed to evaluate the relative protein abundance of Chc in two A339V clones (C1 and C2) at 48 h post-transfection. The corresponding expression levels of cytoplasmic (Cyto) and nuclear (nuclear) p-Stat3 and total Stat3 are shown. β-Tubulin and histone were used as the loading control. (B) BrdU cell proliferation assay was performed on PCLL3 cells at 48 h post-transfection. Relative proliferation rates of Chc knockdown clones (*si-Chc*) and the non-silencing control (*si-NS*) with or without the overexpression of Chc are shown in the bar chart. (C) Western blot analysis was performed to evaluate the relative abundance of total pStat3, cytoplasmic, and nuclear pStat3 in of PCCL3 transfectants overexpressing EGFP or Chc-DN (1-479). Actin was used as the loading control. (D) BrdU cell proliferation assay was performed on pEGFP and CHC-DN overexpressing cells at 48 h post-transfection. Relative proliferation rates of these cells are shown in the bar chart. Bars bearing different letters (a, b, c) are statistically different (by ANOVA, $p < 0.05$). NS: not statistically different.

CHC expression and STAT3 signaling activation in MNG development, and additional hits or factors are likely required for the development of PTC. Table 2 compares the characteristics between patients with MNG and with PTC. Age at operation, clinical presentation, history of thyroid surgery or thyrotoxicosis, and size of excised thyroid tissues between the two groups were comparable.

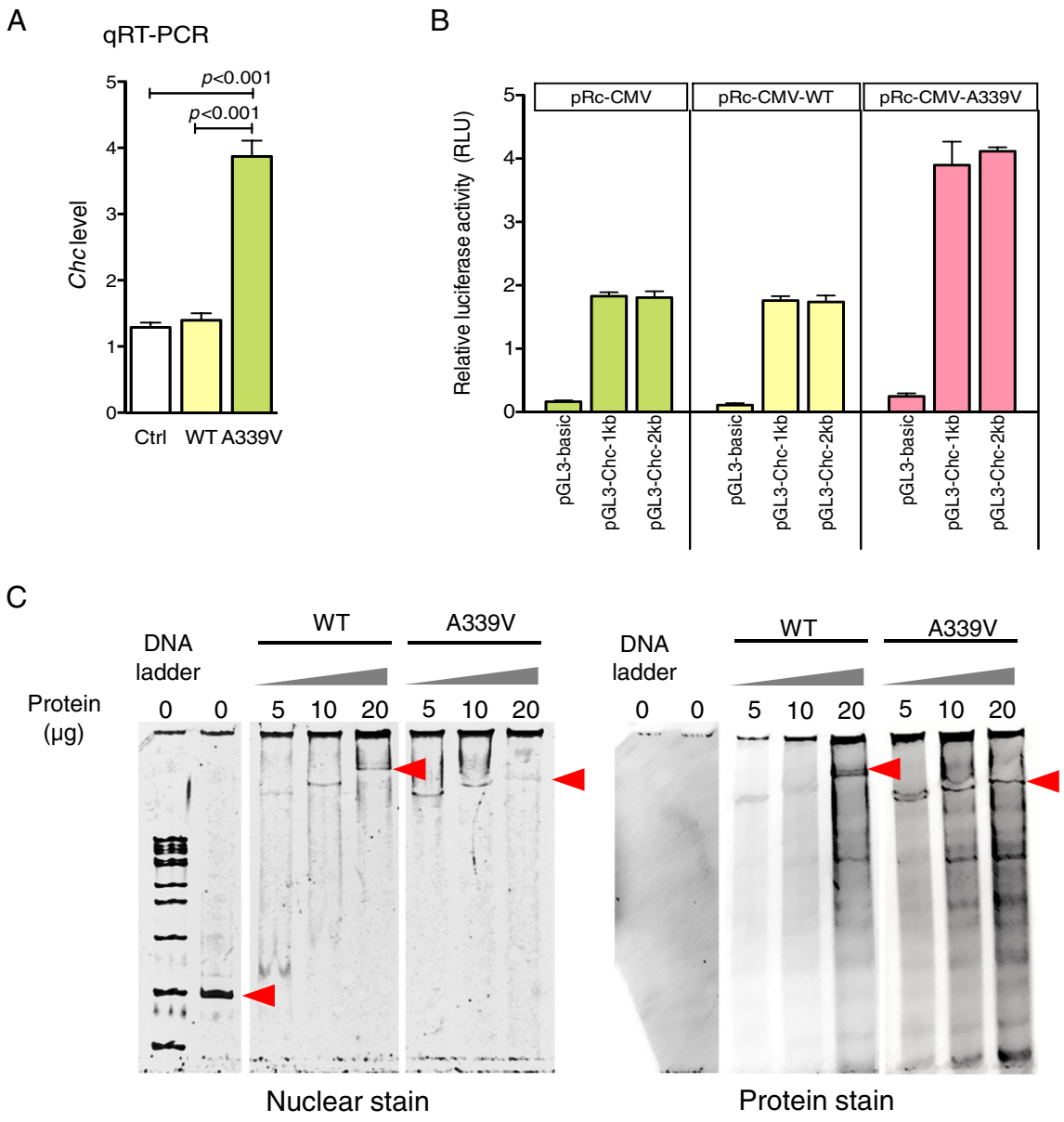

Fig. 5. A339V TTF1 aberrantly transactivates *Chc* gene expression. (A) The expression levels of Chc in PCCL3 clones were measured by real-time PCR, and expression was normalized to that of 18S mRNA. Data were presented as the relative fold changes relative to the *Chc* RNA level of PCCL3 transfected with pCR/CMV (Ctrl). (B) Luciferase reporter assays were performed to compare the transactivation activities of the WT and A339V TTF1 on the *Chc* promoter. A reporter plasmid encoding luciferase under the control of *Chc* promoter, pGL3-Chc, was transfected into Cos-7 cells along with an internal control plasmid encoding *Renilla* luciferase pRL-SV40. Promoter activities are expressed as relative luciferase activity after normalization to *Renilla* activities. *p* values less than 0.05 were deemed to be statistically significant (*). (C) EMSA were performed with nuclear proteins extracted from PCCL3 cells transfected with wild-type or A339V TTF1 and the proximal 1 kb *Chc* promoter. The DNA probes and protein were detected using nuclear and protein stain as indicated. Arrow heads mark the shifted bands.

4. Discussion

In thyroid cells with an ectopic expression of A339V TTF1, Stat3 has been shown to be aberrantly phosphorylated and is believed to be the major survival signal in these cells [7]. In this study, we further delineated a possible role of EGF/Chc/STAT3 signaling in MNG development. We demonstrated that A339V mutation substantially perturbs gene-specific transactivation activity of TTF1 and results in an aberrant expression of *Chc*. Chc is a major component of CME which mediates cellular material uptake and trafficking. Chc is ubiquitously expressed in normal tissues, while its pathological role in human diseases is still not clear. With thyroid cells overexpressing A339V TTF1, we showed that elevated Chc promotes Egfr recycling as well as activation of Stat3 pathway, one of the major EGF downstream pathways, which may cause a prolonged EGF signaling and enhance EGF-dependent biological responses [15]. As matter of fact that, the Stat3 pathway is consistently activated in A339V clones and MNG samples, closely associated with Chc expression. More importantly, our data also indicated that elevated Chc expression facilitates the translocation of pStat3 from cytoplasm to nuclear, which is essential for pStat3 to turn on its downstream target genes. Both the increased Egfr recycling and nuclear localization of pStat3 allow thyroid cells to gain proliferative advantages and hormone independence, representing an initiation step of cellular transformation.

Increasing evidence suggests that aberrant cargo transported by CME may lead to a constitutive activation of survival signals favoring tumorigenesis. At cell junctions, CME is also implicated in integrin internalization and an aberrant CME increases cell invasiveness [20]. So far, Chc has been reported to have its expression changed only in hepatocellular carcinoma [21,22]. Our expression profiling analysis of Chc on MNG and PTC samples (with wild-type *TITF1*) showed that Chc is only

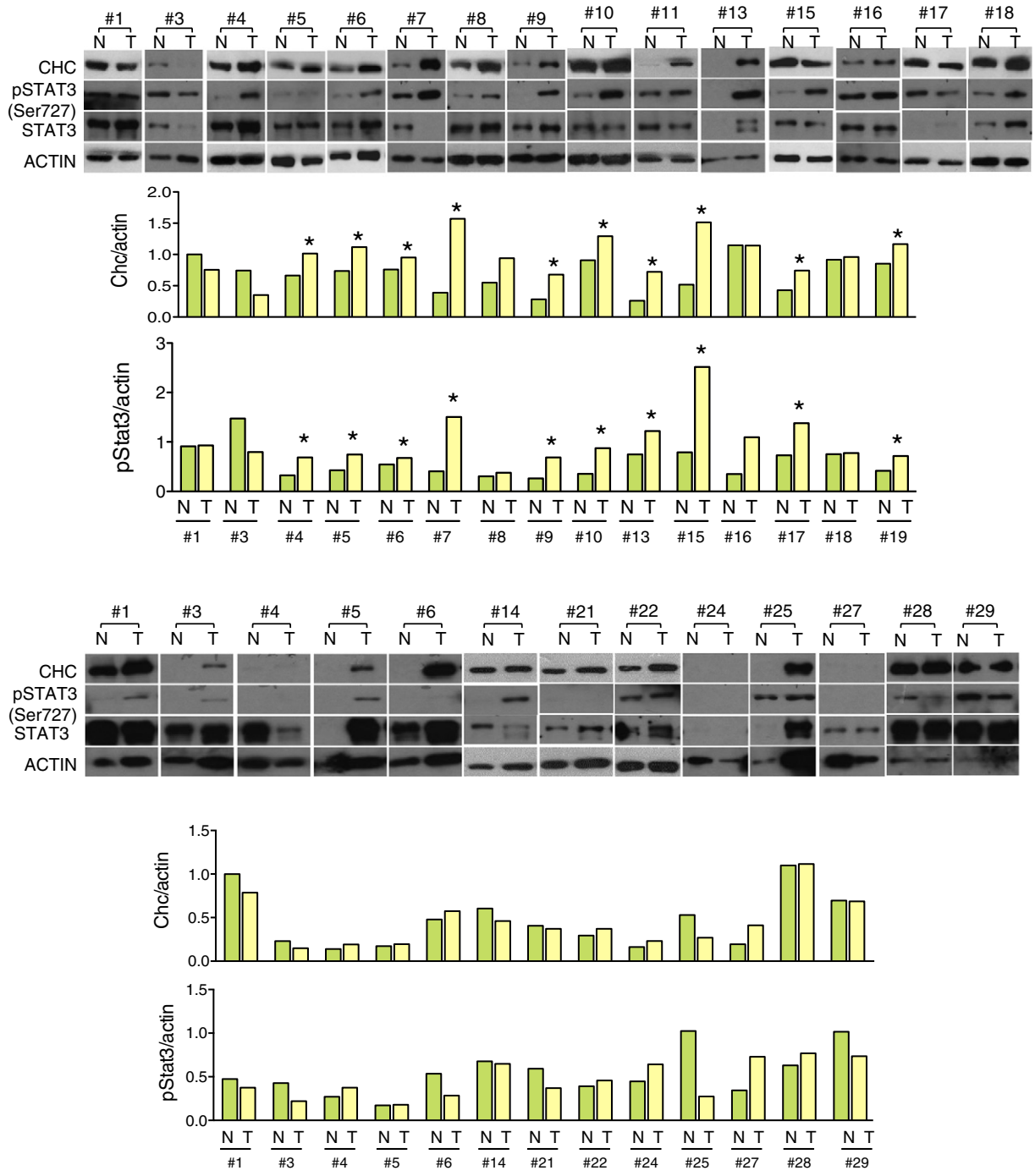

Fig. 6. Perturbed expression of CHC and pSTAT3 in MNG. Western blot analysis was performed in (A) 15 MNG, (B) 13 PTC primary tumors, and the corresponding adjacent thyroid/non-tumor tissues. Actin was used as the loading control. Bands were quantified by densitometry and their normalized values are shown in the bar charts. The co-overexpression of CHC and pSTAT3 were found in 10/15 MNG samples marked with "*".

up-regulated in the pre-malignant thyroid tissues. It may suggest that the elevated expression of Chc and pSTAT3 by A339V TTF1 only represents an early event that contributes to the development of MNG. Other effects triggered by the expression of the mutant TTF1 and/or the second hit that occurred during perturbed cell growth are likely required for the development of PTC. Indeed, multiple genes and pathways were found to be affected by the A339V mutation. A339V TTF1 perturbed the expressions of the varied thyroid genes, including thyrotropin receptor (TSH-R) and thyroglobulin (TG), which work synergistically to mediate differentiation of thyroid cells [23]. The perturbation of differentiation signals perhaps further prompted the aberrant growth of thyroid cells. In addition, STAT3 activation was associated with the cytoplasmic localization of p53, which has been suggested as a risk factor for the development of neoplastic diseases [24]. A slight alternation of p53 pathway was also observed in our proteomic pathway data. This also raised the possibility that perturbed p53 pathway could favor the accumulation of somatic mutations in these rapidly dividing thyroid cells, favoring disease progression. In particular, we found elevated pSTAT3 expression is highly correlated with CHC overexpression in MNG samples; it is conceivable that those factors or signals regulating STAT3 signaling would be responsible for the sustainable growth of pre-malignant thyroid cells and favor the PTC development. In other

Table 2
A comparison of characteristics between patients with benign multinodular goiter (MNG) and with papillary thyroid carcinoma (PTC).

	MNG ($n = 15$)	PTC ($n = 13$)	p-value[a]
Age of diagnosis in years, median [range]	61.0 (30.0–90.0)	48.0 (8.0–82.0)	0.65
Sex (male/female)	1 / 14	4 / 9	0.09
History of thyroid surgery, no. [%]	1 [6.7]	1 [7.7]	1.000
History of thyrotoxicosis, no. [%]	1 [6.7]	0 [0.0]	1.000
Weight of excised thyroid gland in grams, median [range]	21.0 [14.4–59.0]	21.0 [4.5–50.0]	0.519
Tumor size (cm)	3.0 (0.5–5.5)	1.5 (0.3–5.0)	0.065
Tumor multifocality	–	7 [53.8]	–
Tumor stage grouping			
- T1 N0 M0	–	2 [15.4]	–
- T1 N1b M0	–	1[7.7]	–
- T2 N0 M0	–	1 [7.7]	–
- T2 N1b M0	–	4 [30.8]	–
- T4 N0 M0	–	1 [7.7]	–
- T4 N1b M0	–	3 [23.1]	–
- T4 N1b M1	–	1 [7.7]	–
CHC overexpression, no.[%]	11 [73.3]	0 [0.0]	<**0.001**
pSTAT3 overexpression, no.[%]	11 [73.3]	0 [0.0]	<**0.001**

Abbreviation: CHC = clathrin heavy chain.
P values indicated in bold show the significant difference between two groups.
[a] By Fisher-exact or Mann–Whitney *U*-tests.

words, cumulative effects of all these perturbed pathways could contribute to the pathogenesis of MNG and/or PTC.

In summary, our report here provides the first evidence showing that an up-regulated level of Chc promotes cellular transformation of thyroid cells by enhancing CME-dependent Egfr recycling and transport of pStat3. In addition, our findings offer a broader spectrum of points of intervention and also provide relevant insights to the risk assessment or prevention measure for MNG.

Supplementary data to this article can be found online at http://dx.doi.org/10.1016/j.bbadis.2015.05.005.

Transparency documents

The Transparency documents associated with this article can be found, in online version.

Disclosures

The authors declare no conflict of interest.

Acknowledgement

This work was supported by the research grant HKU 772808M from the Hong Kong Research Grants Council to ESW Ngan and the Special Equipment Grant from the University Grants Committee of the Hong Kong (Project Code: SEG_HKU02) to CM Che.

References

[1] N. Arora, T. Scognamiglio, B. Zhu, T.J. Fahey 3rd, Do benign thyroid nodules have malignant potential? An evidence-based review, World J. Surg. 32 (2008) 1237–1246.
[2] R.F. Grossman, S.H. Tu, Q.Y. Duh, A.E. Siperstein, F. Novosolov, O.H. Clark, Familial nonmedullary thyroid cancer. An emerging entity that warrants aggressive treatment, Arch. Surg. 130 (1995) 892–897 (discussion 898–899).
[3] T.J. Musholt, P.B. Musholt, T. Petrich, G. Oetting, W.H. Knapp, J. Klempnauer, Familial papillary thyroid carcinoma: genetics, criteria for diagnosis, clinical features, and surgical treatment, World J. Surg. 24 (2000) 1409–1417.
[4] A. Pucci, M. Suppo, G. Lucchesi, A. Celeste, L. Viberti, R. Pellerito, M. Papotti, Papillary thyroid carcinoma presenting as a solitary soft tissue arm metastasis in an elderly hyperthyroid patient. Case report and review of the literature, Virchows Arch. 448 (2006) 857–861.
[5] S. Uchino, S. Noguchi, H. Kawamoto, H. Yamashita, S. Watanabe, S. Shuto, Familial nonmedullary thyroid carcinoma characterized by multifocality and a high recurrence rate in a large study population, World J. Surg. 26 (2002) 897–902.
[6] J.R. Burgess, A. Duffield, S.J. Wilkinson, R. Ware, T.M. Greenaway, J. Percival, L. Hoffman, Two families with an autosomal dominant inheritance pattern for papillary carcinoma of the thyroid, J. Clin. Endocrinol. Metab. 82 (1997) 345–348.
[7] E.S. Ngan, B.H. Lang, T. Liu, C.K. Shum, M.T. So, D.K. Lau, T.Y. Leon, S.S. Cherny, S.Y. Tsai, C.Y. Lo, U.S. Khoo, P.K. Tam, M.M. Garcia-Barcelo, A germline mutation (A339V) in thyroid transcription factor-1 (TITF-1/NKX2.1) in patients with multinodular goiter and papillary thyroid carcinoma, J. Natl. Cancer Inst. 101 (2009) 162–175.
[8] G. Vassart, J.E. Dumont, The thyrotropin receptor and the regulation of thyrocyte function and growth, Endocr. Rev. 13 (1992) 596–611.
[9] L.M. Asmis, H. Gerber, J. Kaempf, H. Studer, Epidermal growth factor stimulates cell proliferation and inhibits iodide uptake of FRTL-5 cells in vitro, J. Endocrinol. 145 (1995) 513–520.
[10] T. Hoelting, A.E. Siperstein, O.H. Clark, Q.Y. Duh, Epidermal growth factor enhances proliferation, migration, and invasion of follicular and papillary thyroid cancer in vitro and in vivo, J. Clin. Endocrinol. Metab. 79 (1994) 401–408.
[11] J. Zhang, A. Gill, B. Atmore, A. Johns, L. Delbridge, R. Lai, T. McMullen, Upregulation of the signal transducers and activators of transcription 3 (STAT3) pathway in lymphatic metastases of papillary thyroid cancer, Int. J. Clin. Exp. Pathol. 4 (2011) 356–362.
[12] G. Mincione, M.C. Di Marcantonio, C. Tarantelli, S. D'Inzeo, A. Nicolussi, F. Nardi, C.F. Donini, A. Coppa, EGF and TGF-beta1 effects on thyroid function, J. Thyroid. Res. 2011 (2011) 431718.
[13] R. DeLellis, R. Lloyd, P. Heitz, C. Eng, World Health Organization Classification of Tumors: Pathology and Genetics of Tumors of Endocrine Organs, WHO Press, 2004.
[14] C. Li, N.L. Zhu, R.C. Tan, P.L. Ballard, R. Derynck, P. Minoo, Transforming growth factor-beta inhibits pulmonary surfactant protein B gene transcription through SMAD3 interactions with NKX2.1 and HNF-3 transcription factors, J. Biol. Chem. 277 (2002) 38399–38408.
[15] S. Sigismund, E. Argenzio, D. Tosoni, E. Cavallaro, S. Polo, P.P. Di Fiore, Clathrin-mediated internalization is essential for sustained EGFR signaling but dispensable for degradation, Dev. Cell 15 (2008) 209–219.
[16] A.H. Bild, J. Turkson, R. Jove, Cytoplasmic transport of Stat3 by receptor-mediated endocytosis, EMBO J. 21 (2002) 3255–3263.
[17] M. Shah, K. Patel, S. Mukhopadhyay, F. Xu, G. Guo, P.B. Sehgal, Membrane-associated STAT3 and PY-STAT3 in the cytoplasm, J. Biol. Chem. 281 (2006) 7302–7308.
[18] S.J. Royle, N.A. Bright, L. Lagnado, Clathrin is required for the function of the mitotic spindle, Nature 434 (2005) 1152–1157.
[19] Y. Maeda, T. Tsuchiya, H. Hao, D.H. Tompkins, Y. Xu, M.L. Mucenski, L. Du, A.R. Keiser, T. Fukazawa, Y. Naomoto, T. Nagayasu, J.A. Whitsett, Kras(G12D) and Nkx2-1 haploinsufficiency induce mucinous adenocarcinoma of the lung, J. Clin. Invest. 122 (2012) 4388–4400.
[20] A.G. Ramsay, M.D. Keppler, M. Jazayeri, G.J. Thomas, M. Parsons, S. Violette, P. Weinreb, I.R. Hart, J.F. Marshall, HS1-associated protein X-1 regulates carcinoma cell migration and invasion via clathrin-mediated endocytosis of integrin alphavbeta6, Cancer Res. 67 (2007) 5275–5284.
[21] M. Seimiya, T. Tomonaga, K. Matsushita, M. Sunaga, M. Oh-Ishi, Y. Kodera, T. Maeda, S. Takano, A. Togawa, H. Yoshitomi, M. Otsuka, M. Yamamoto, M. Nakano, M. Miyazaki, F. Nomura, Identification of novel immunohistochemical tumor markers for primary hepatocellular carcinoma; clathrin heavy chain and formiminotransferase cyclodeaminase, Hepatology 48 (2008) 519–530.
[22] H. Uto, S. Kanmura, Y. Takami, H. Tsubouchi, Clinical proteomics for liver disease: a promising approach for discovery of novel biomarkers, Proteome Sci. 8 (2010) 70.
[23] P. Roger, M. Taton, J. Vansande, J.E. Dumont, Mitogenic effects of thyrotropin and adenosine-3′,5′-monophosphate in differentiated normal human thyroid-cells invitro, J. Clin. Endocrinol. Metab. 66 (1988) 1158–1165.
[24] G. Ardito, L. Revelli, A. Boninsegna, A. Sgambato, F. Moschella, M.C. Marzola, E. Giustozzi, N. Avenia, M. Castelli, D. Rubello, Immunohistochemical evaluation of inflammatory and proliferative markers in adjacent normal thyroid tissue in patients undergoing total thyroidectomy: results of a preliminary study, J. Exp. Clin. Cancer Res. 29 (2010) 77.